REVISTA DCS
FUNDADA EN 2000

# TUNING THE RAMAN AND ELECTRONIC PROPERTIES OF GRAPHENE QUANTUM DOTS THROUGH ALKALI-ION ADSORPTION: A DFT STUDY

## ASSINATURAS RAMAN E ALTERAÇÕES ELETRÔNICAS DE GQDS INDUZIDAS PELA ADSORÇÃO DE ÍONS ALCALINOS: UM ESTUDO UTILIZANDO DFT

## AJUSTE DE LAS PROPIEDADES RAMAN Y ELECTRÓNICAS DE LOS PUNTOS CUÁNTICOS DE GRAFENO MEDIANTE LA ADSORCIÓN DE IONES ALCALINOS: UN ESTUDIO DFT

**Tharles Antônio Ribeiro[1], Ana Isabela Pianowski Salussoglia[2], Ericson Hamisses Nunes Souza Thaines[3], Rafael Felipe Vicentini[4], Renato Garcia de Freitas Sobrinho[5]**

**DOI:** 10.54899/dcs.v22i85.3978
**Recibido: 07/12/2025 | Aceptado: 08/12/2025 | Publicación en línea: 26/12/2025.**

## ABSTRACT

Understanding how alkali ions influence the vibrational and electronic properties of graphene quantum dots (GQDs) is essential for advancing carbon-based materials in electrochemical applications. In this study, density functional theory (DFT) simulations were performed to evaluate the effects of $Li^+$, $Na^+$, and $K^+$ adsorption on GQDs. Raman analysis revealed systematic shifts in the D and G bands, consistent with trends observed in *operando* experiments. Among the investigated systems, GQD#$Li^+$ exhibited the strongest interactions, including a D-band shift of +2.04 $cm^{-1}$, the highest ID/IG ratio, and the most favorable adsorption energy (−2.18 eV). Frontier orbital and electron density analyses showed significant charge redistribution and modulation of HOMO, LUMO, and Fermi levels upon ion adsorption. Overall, the results indicate that alkali ions effectively tune the structural and electronic properties of GQDs, with lithium demonstrating the greatest potential for applications in energy storage, interfacial ion modulation, and nanoscale sensing.

**Keywords:** Graphene Quantum Dots. Raman. Density Functional Theory.

## RESUMO

Compreender como os íons alcalinos influenciam as propriedades vibracionais e eletrônicas de

[1] PhD in Electrical Engineering, Universidade Estadual de Campinas (UNICAMP), Campinas, São Paulo, Brazil. E-mail: tharlesmg@gmail.com Orcid: https://orcid.org/0000-0002-6347-9210
[2] PhD in Chemical Engineering, Universidade Estadual de Campinas (UNICAMP), Campinas, São Paulo, Brazil. E-mail: anaips@unicamp.br Orcid: https://orcid.org/0000-0002-0936-1449
[3] PhD in Chemistry, Universidade Federal do Mato Grosso (UFMT), Cuiabá, Mato Grosso, Brazil. E-mail: hamissesufmt@gmail.com Orcid: https://orcid.org/0000-0002-0142-5276
[4] PhD in Electrical Engineering, Universidade Estadual de Campinas (UNICAMP), Campinas, São Paulo, Brazil. E-mail: rafael.vicentini22@gmail.com Orcid: https://orcid.org/0000-0001-6906-8669
[5] PhD in Chemistry, Universidade Federal do Mato Groso (UFMT), Cuiabá, Mato Grosso, Brazil. E-mail: renato.sobrinho@ufmt.br Orcid: https://orcid.org/0000-0003-4480-7212

pontos quânticos de grafeno (GQDs) é fundamental para o avanço de materiais à base de carbono em aplicações eletroquímicas. Neste estudo, simulações baseadas em teoria do funcional da densidade (DFT) foram realizadas para avaliar os efeitos da adsorção de $Li^+$, $Na^+$ e $K^+$ em GQDs. A análise Raman revelou deslocamentos sistemáticos nas bandas D e G, consistentes com tendências observadas em experimentos *operando*. Entre os sistemas investigados, o GQD#$Li^+$ apresentou as interações mais fortes, incluindo um deslocamento de +2,04 $cm^{-1}$ na banda D, o maior índice de desordem ID/IG e a energia de adsorção mais favorável (−2,18 eV). As análises dos orbitais de fronteira e da densidade eletrônica mostraram redistribuição significativa de carga e modulação dos níveis de HOMO, LUMO e Fermi após a adsorção. No geral, os resultados indicam que íons alcalinos modulam eficazmente as propriedades estruturais e eletrônicas dos GQDs, com o lítio apresentando maior potencial para aplicações em armazenamento de energia, modulação interfacial e nanosensoriamento.

**Palavras-chave:** Pontos Quânticos de Grafeno. Raman. Teoria do Funcional da Densidade.

**RESUMEN**

Comprender cómo los iones alcalinos influyen en las propiedades vibracionales y electrónicas de los puntos cuánticos de grafeno (GQDs) es fundamental para el avance de los materiales basados en carbono en aplicaciones electroquímicas. En este estudio, se realizaron simulaciones de teoría del funcional de la densidad (DFT) para evaluar los efectos de la adsorción de $Li^+$, $Na^+$ y $K^+$ en los GQDs. El análisis Raman reveló desplazamientos sistemáticos en las bandas D y G, consistentes con las tendencias observadas en experimentos operando. Entre los sistemas investigados, GQD#$Li^+$ mostró las interacciones más fuertes, incluyendo un desplazamiento de la banda D de +2.04 $cm^{-1}$, la mayor razón ID/IG y la energía de adsorción más favorable (−2.18 eV). Los análisis de los orbitales frontera y de la densidad electrónica evidenciaron una redistribución significativa de carga y una modulación de los niveles HOMO, LUMO y de Fermi tras la adsorción iónica. En conjunto, los resultados indican que los iones alcalinos ajustan de manera efectiva las propiedades estructurales y electrónicas de los GQDs, destacándose el litio por su mayor potencial en aplicaciones de almacenamiento de energía, modulación interfacial de iones y sensado a escala nanométrica.

**Palabras clave:** Puntos Cuánticos de Grafeno. Raman. Teoría del Funcional de la Densidad.



## INTRODUCTION

The intensification of global energy challenges has driven the pursuit of more effective and sustainable energy storage solutions. In this context, supercapacitors emerge as ideal alternatives due to their low cost, long cycle life, high power density, and outstanding cycling stability (CAI; MOMEN; *et al*., 2021; CAI; ZOU; *et al*., 2021; ZHANG *et al*., 2014; ZOU *et al*.,

2021). These characteristics make them promising not only for conventional applications but also for integrating renewable energy systems and smart grids, thereby contributing to the global energy transition. The choice of electrode material has a direct impact on its electrochemical properties. Therefore, for the development of high-performance supercapacitors, it is crucial to explore new materials that not only optimize charge storage capacity but also ensure higher energy efficiency and long-term stability (DENG *et al*., 2021).

In the current context, nanostructured materials such as graphene quantum dots (GQDs) emerge as a promising option to meet the increasing demand for advanced energy storage solutions. GQDs exhibit a range of distinct characteristics that make them particularly suitable for applications in supercapacitors and other next-generation energy storage devices (XIAO; MOMEN; LIU, 2021). Among these characteristics, notable features include the remarkable surface area, which significantly enhances the electrical charge storage capacity, graphene's exceptional electrical conductivity that allows efficient electron transfer during charge and discharge processes, robust structural stability ensuring durability and resistance to repeated cycles, ease of manufacturing and functionalization enabling precise adjustments to material properties as required by specific applications, and environmental compatibility, promoting sustainable practices in energy storage technology production (GUO *et al*., 2021; LI, Lin *et al*., 2021; XIAO; MOMEN; LIU, 2021).

Raman spectroscopy is an important technique for investigating the properties of carbon nanostructures, as well as their structure and electronic characteristics (LEE *et al*., 2012; LIU, J. *et al*., 2013; TUNG *et al*., 2023; WANG, H. *et al*., 2014). In this context, the main bands of graphene were G and D. The G band, around 1580 $cm^{-1}$, reflects the planar vibration of $sp^2$ carbon atoms in the graphene structure (COMPAGNINI *et al*., 2011; LEE *et al*., 2012; WANG, H. *et al*., 2014; WANG, Y. ying *et al*., 2008) and the D band, around 1200–1350 $cm^{-1}$, is associated with structural defects and disturbances located near defects or edges of graphene (COMPAGNINI *et al*., 2011; MALARD *et al*., 2009; SIMON; GOGOTSI, 2020; TUNG *et al*., 2023; WU *et al*., 2018a).

The integration of Raman spectroscopy with in operando techniques represents a robust and insightful methodology for characterizing graphene-based materials during the charging and discharging processes of supercapacitors. This combined approach facilitates the real-time monitoring of structural and electronic transformations within the material under various polarization conditions. Despite the recognized utility of this technique, there remains a

substantial gap in the literature concerning a comprehensive understanding of the behavior of the G and D bands in the Raman spectra of graphene during dynamic operational regimes. While it is well established that these bands are acutely sensitive to structural modifications, the degree of disorder, and the presence of defects, the precise impact of direct interactions between electrolyte ions and graphene on the spectral shifts and intensity changes of these bands throughout the charge–discharge cycles has yet to be thoroughly elucidated.

In this context, the fundamental role of computational simulations in contemporary research becomes evident, particularly those based on density functional theory (DFT). The use of programming and modeling tools enables a rigorous initial screening of materials and phenomena, thereby optimizing experimental design and conserving time and resources that would otherwise be expended in purely experimental approaches. DFT, in particular, offers notable advantages, such as its ability to provide detailed descriptions of electronic interactions and vibrational properties at the atomic level. This theoretical framework delivers predictive insights into the behavior of the G and D bands of graphene in the presence of various ionic species at the electrode/electrolyte interface of supercapacitors under operational conditions (CAPELLE, 2006; DAVID S. SHOLL; JANICE A. STECKEL, 2009)

This work performed a theoretical study of GQD and GQD modified by the adsorption of $Li^+$, $Na^+$, and $K^+$ ions, using density functional theory (DFT) simulations to understand the shift in the G and D bands during Raman analysis operating in supercapacitors. The Raman spectrum simulation was carried out using the Gaussian software with the CAM-B3LYP exchange-correlation functional and a 6-311++G basis set, while the energy shift calculations were performed using the Quantum ESPRESSO software (BPE and PAH). The simulation considers the atomic structure of the material and predicts the behavior of the HOMO, LUMO, and Fermi energies.

## EXPERIMENTAL PROCEDURE

For this study, all simulations with GQD were performed using the Gaussian 16 software(FRISCH, M. J. *et al*., 2009) employing Density Functional Theory (DFT) methodology (FRISCH, Michael J.; POPLE; BINKLEY, 1984; KOHN; SHAM, 1965). Initially, a graphene sheet was optimized in vacuum using the CAM-B3LYP exchange-correlation functional and a 6-311++G(d,p) basis set (FRISCH, Michael J.; POPLE; BINKLEY, 1984; YANAI; TEW;

HANDY, 2004). The initial geometry of the graphene sheet was optimized. Subsequently, lithium, sodium, and potassium ions were individually added to the GQDs. The simulations were re-optimized to compute vibrational frequencies and subjected to DFT quantum mechanics calculations at the CAM-B3LYP/6-311++G(d,p) level. During geometry optimization, it was observed that there were no imaginary frequency modes, indicating that the simulations reached minimum energy points. To correlate theoretical results with experimental data, scaling factors were adjusted using a correction factor (KASHINSKI *et al*., 2017). Starting from the optimized simulations, results from Raman spectroscopy were obtained, including analysis of the D and G bands, as well as the electronic structure of the systems under study. The intensity ratios between the D and G modes are a significant characteristic of graphene structures. Specifically, the ID/IG ratio (where ID and IG represent the intensities of the D and G bands, respectively) is a crucial parameter related to the defect density in the graphene crystal lattice (FERRARI; BASKO, 2013). The frontier orbitals (HOMO/LUMO) were simulated using the same functional and basis set for each ion-GQD system, providing a detailed characterization of the electronic and structural properties of these materials. The results for the density of states and Fermi energy were extracted using the Multiwfn software (LU; CHEN, 2012).

All simulations for periodic graphene were performed using the Quantum ESPRESSO software package. Structural optimization was carried out through stationary point energy (SCF) calculations, followed by computations of electronic density, band structure, and density of states. Additionally, theoretical Raman spectroscopy spectra were obtained, with particular attention given to the analysis of the D and G bands. The atomic coordinates of pristine graphene were defined using a 4×4 supercell containing 32 carbon atoms arranged in a hexagonal lattice, with a C–C bond length of 1.421 Å and a bond angle of 120°, in accordance with values reported in the literature and recent studies based on density functional theory (DFT).(TAYYAB *et al*., 2020).

The intensity ratios between the D and G modes are a significant characteristic of graphene structures. Specifically, the

$$\frac{ID}{IG} \qquad (1)$$

where

ID and IG represent the intensities of the D and G bands, respectively, is a crucial parameter related to the defect. density in the graphene crystal lattice(FERRARI; BASKO, 2013).

From the optimization, the total adsorption energy $\Delta E_{ads}$ was calculated for each structure according to the equation:

$$\Delta E_{ads} = E_{x+\#G} - (E_G + E_{x+}) \quad (2)$$

where

$E_{x+\#G}$ is the total energy of each structure after ionic adsorption, $E_G$ is the total energy of isolated graphene structures and $E_{x+}$ corresponds to the ion's total energy.

The Highest Occupied Molecular Orbital (HOMO) and Lowest Unoccupied Molecular Orbital (LUMO) were simulated using the same functional and basis set for each ion-GQD system, providing a detailed characterization of the electronic and structural properties of these materials.

## RESULTS AND DISCUSSIONS

The Raman spectra obtained through DFT simulations were performed for GQD and GQD modified by the adsorption of $Li^+$, $Na^+$, and $K^+$ ions, respectively, named GQD#$Li^+$, GQD#$Na^+$, and GQD#$K^+$. The comparison between GQDs and GQD#$Li^+$, GQD#$Na^+$, and GQD#K can be seen in **Figure 1 (a-c)**, respectively. The simulations provided valuable insights into how ion adsorption alters the behavior of the D and G bands in the Raman spectrum of graphene, as well as the electron density distributions and frontier molecular orbitals, enabling a direct correlation among these properties.

Figure 1. Comparison between Raman Spectra of GQD and (a) GQD#$Li^+$, (b) GQD#$Na^+$, and (c) GQD#$K^+$.

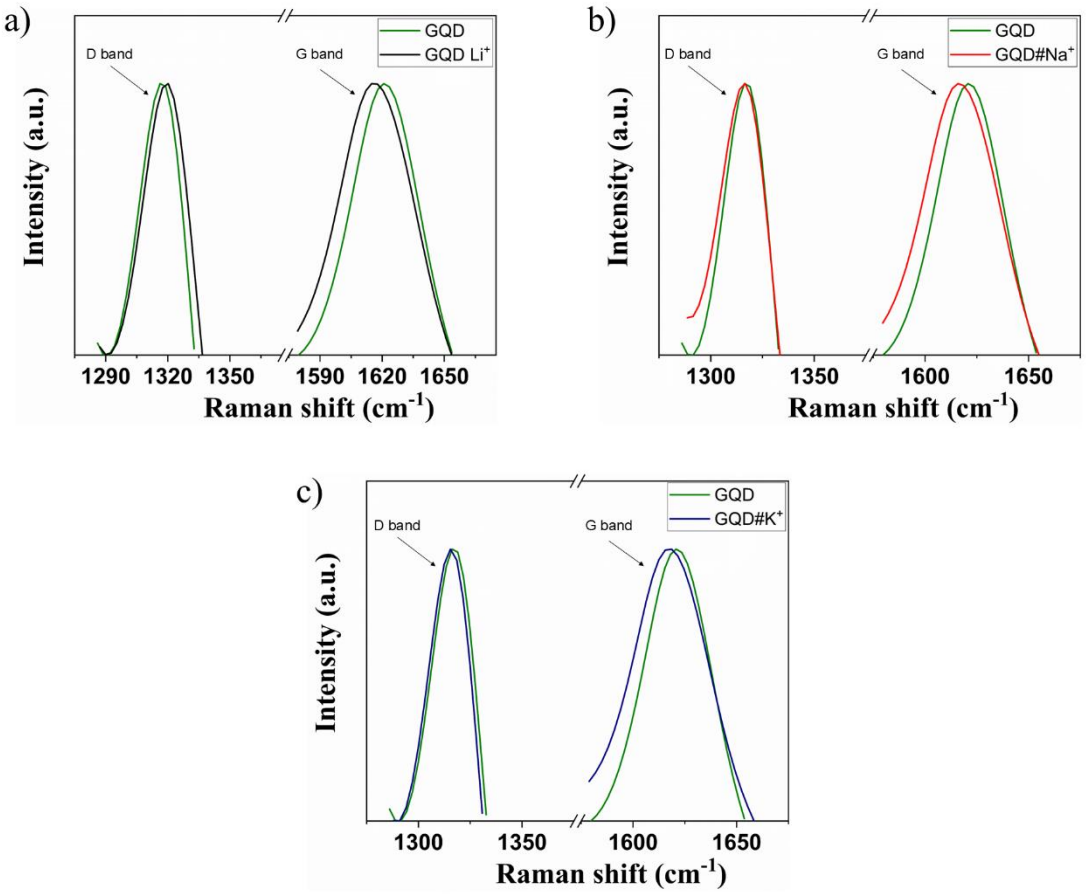


Source: Authors.

**Table 1** shows the detailed variation in intensities of the D and G bands, respectively, comparing GQD with the modifications GQD#$Li^+$, GQD#$Na^+$, and GQD#$K^+$. For GQD, the D band was calculated at 1318.62 $cm^{-1}$, and the G band at 1617.55 $cm^{-1}$, values that are consistent with predictions reported by Wu *et al* (WU *et al*., 2018b). GQD#$Li^+$ presents D-band at 1320.66 $cm^{-1}$, and G-band at 1612.10 $cm^{-1}$, showing shifts compared to GQD of 2.04 $cm^{-1}$ and -5.45 $cm^{-1}$, respectively. GQD#$Na^+$ exhibit shifts of -1.05 $cm^{-1}$ for D-band (1317.57 $cm^{-1}$) and of -5.21 $cm^{-1}$ for G-band (1612.34 $cm^{-1}$). Simulations for GQD containing potassium ions display a D band at 1317.23 $cm^{-1}$ and a G band at 1613.33 $cm^{-1}$, with shifts of -1.39 $cm^{-1}$ and -4.22 $cm^{-1}$, respectively.

Many researchers in the field of carbon-based materials are striving to clearly identify and interpret the D and G bands through operando Raman spectroscopy. Despite significant advances, there remains a notable gap in the literature regarding the reliable detection of these bands under operando conditions, largely due to the complex interplay between structural defects, charge transfer, and dynamic interfacial processes. This challenge is widely recognized as fundamental

for understanding material behavior in realistic environments, and addressing it is considered crucial for both fundamental science and the development of advanced electrochemical technologies (BA *et al*., 2022; HONG *et al*., 2013; RABELO *et al*., 2023; VICENTINI; DA SILVA; *et al*., 2021).

In the study by Vicentini *et al*. (2021, *ACS Applied Materials & Interfaces*), polished graphite was employed as an electrode in a highly concentrated aqueous $NaClO_4$ electrolyte (WiSE). Spectroscopic analyses under non-polarized conditions revealed the D band at approximately 1310 $cm^{-1}$ and the G band centered between 1582–1584 $cm^{-1}$. Upon application of potentials up to 1.8 V, a blue shift of the D band of up to +6 $cm^{-1}$ was observed, along with the splitting of the G band towards the 1615 $cm^{-1}$ region ($E_{2G'}$), a phenomenon attributed to ion intercalation within the graphitic layers(VICENTINI; VENÂNCIO; *et al*., 2021). In a complementary study, Vicentini *et al*. (2021, *Journal of Energy Chemistry*) investigated polycrystalline graphite in aqueous $Li_2SO_4$, $Na_2SO_4$, and $K_2SO_4$ electrolytes, finding that the D band varied from 1308 to 1313 $cm^{-1}$ depending on the cation and applied potential, with positive shifts of up to +4 $cm^{-1}$ during dynamic operation, while the G band remained centered between 1580–1585 $cm^{-1}$. The reversible shifts observed during charge/discharge cycles were correlated with modulation of the electrostatic potential at the interface, which is sensitive to the nature of the cation in solution(VICENTINI; DA SILVA; *et al*., 2021).

Several additional experimental studies complement this overview across different carbon materials. Venâncio *et al*. (2022, *Journal of Energy Storage*) compared activated carbon (AC), multiwall carbon nanotubes (MWCNTs), and graphite electrodes using a $TEABF_4$ organic electrolyte. For AC, the D and G bands were found at ~1350 $cm^{-1}$ and ~1580 $cm^{-1}$, respectively, with no significant presence of the 2D band. In MWCNT electrodes, these values were positioned between 1355–1360 $cm^{-1}$ (D) and near 1582 $cm^{-1}$ (G). In the case of graphite electrodes, splitting of the G band was observed (E2G2(i): 1584 $cm^{-1}$, E2G2(b): 1615 $cm^{-1}$), attributed to the intercalation of $BF_4^-$ anions; this splitting was accompanied by gradual shifts under different applied potentials, reflecting adsorption and ion insertion processes(VENÂNCIO *et al*., 2022). Raissa Venâncio *et al*. (2023, *Energy Storage Materials*) also reported Raman spectral variations for AC and MWCNTs in $TEABF_4$/propylene carbonate, where increasing potential led to a blue shift of the D band up to 1366 $cm^{-1}$, demonstrating the impact of local electric fields and ionic adsorption on the vibrational modes of carbon and revealing transient doping mechanisms promoted by electrochemical polarization(VENÂNCIO *et al*., 2023).

The GQD#$Li^+$ material exhibited a D-band shift of 2.04 $cm^{-1}$ relative to the reference material, a value that is in excellent agreement with the findings reported by Vicentini *et al*. In their operando Raman spectroscopy study using 785 nm excitation and an applied potential of 0.4 V in a supercapacitor containing $Li_2SO_4$, they also observed a 2.04 $cm^{-1}$ shift in the D-band (VICENTINI; DA SILVA; *et al*., 2021).

The GQD#$Na^+$ material exhibited a shift of -1.05 $cm^{-1}$ in the D-band, positioning it at 1317.57 $cm^{-1}$. Similar results were reported by Weaving *et al*., who, using operando Raman spectroscopy during sodiation and desodiation processes in sodium hard carbon cells, also observed that the D-band is located near 1317 $cm^{-1}$ during both the charging and discharging steps (WEAVING *et al*., 2020).

The simulations performed for GQD containing potassium ions revealed the D-band at 1317.23 $cm^{-1}$, corresponding to a shift of -1.39 $cm^{-1}$ relative to the reference material. A similar result was reported by Vicentini *et al*., who observed a shift of approximately -1 $cm^{-1}$ in the D-band when employing operando Raman spectroscopy with 514 nm excitation under an applied voltage of 1 V in supercapacitors containing $K_2SO_4$ (VICENTINI; DA SILVA; *et al*., 2021).

The intensity ratio between the D and G bands, $I_D/I_G$, serves as an indicator to estimate the degree of disorder and the presence of structural defects in the material (FERRARI; BASKO, 2013; LEE *et al*., 2012). **Table 1** shows the $I_D/I_G$ ratio of GQD, GQD#$Li^+$, GQD#$Na^+$, and GQD#$K^+$. The disorder ratios for GQD, GQD#$Li^+$, GQD#$Na^+$, and GQD#$K^+$ were 0.30, 0.36, 0.33, and 0.31, respectively. GQD is a material with high crystallinity, and the results indicate that cations have a slightly higher disorder ratio compared to GQD. The adsorption energy of each ionic species adsorbed on the GQD surface was calculated using **Equation 1**, as shown in **Table 1**. The adsorption energy was determined for lithium, sodium, and potassium ions, presenting values of -2.18, -1.51, and -1.15 eV, respectively. Lithium ions induced stronger electrostatic interactions due to their higher nuclear charge and smaller ionic radius. Consequently, lithium ions show a greater affinity with the graphene surface compared to sodium and potassium ions, making lithium the most suitable ion for applications in nanostructured energy storage devices (CHMIOLA *et al*., 2010; LI, Linlin *et al*., 2013; LIU, W. *et al*., 2020; PATTARAPONGDILOK; PARASUK, 2020).

Table 1. Raman Shift of D and G band, $I_D/I_G$, and adsorption energy of GQD, GQD#$Li^+$, GQD#$Na^+$, and GQD#$K^+$.

| | GQD | GQD#$Li^+$ | GQD#$Na^+$ | GQD#$K^+$ |
|---|---|---|---|---|
| Raman Shift of D band ($cm^{-1}$) | 1318.62 | 1320.66 | 1317.57 | 1317.23 |
| Raman Shift of G band ($cm^{-1}$) | 1617.55 | 1612.10 | 1612.34 | 1613.33 |
| $I_D/I_G$ | 0.30 | 0.36 | 0.33 | 0.31 |
| Adsorption Energy (eV) | - | -2.18 | -1.51 | -1.15 |

Source: Authors.

The Highest Occupied Molecular Orbital (HOMO) and Lowest Unoccupied Molecular Orbital (LUMO) frontier molecular orbitals allow visualization of lithium, sodium, and potassium ions interacting on the graphene surface (SIMON; GOGOTSI, 2020; XU *et al*., 2011; ZHAO *et al*., 2018). Variations in the Fermi energy can alter the density of states available for electronic transitions, directly affecting phonon normalization and, consequently, the frequencies observed in the D and G bands of the Raman spectrum (LEE *et al*., 2012; MADITO, 2021; XU *et al*., 2011). **Table 2** shows the variations in the energy levels of the HOMO, LUMO, and Fermi for the materials GQD#$Li^+$, GQD#$Na^+$, and GQD#$K^+$. GQD exhibits a HOMO of -6.20 eV, a LUMO of -1.52 eV, and a Fermi of -3.86 eV, resulting in an energy gap of 4.67 eV, which characterizes it as a semiconductor. The addition of lithium shifted the HOMO to -8.84 eV, the LUMO to -4.19 eV, and the Fermi to -6.52 eV. Similarly, sodium incorporation resulted in a HOMO of -8.70 eV, a LUMO of -4.06 eV, and a Fermi of -6.38 eV. The addition of potassium showed a HOMO of -8.61 eV, a LUMO of -3.96 eV, and a Fermi of -6.28 eV. Comparing the data, it was possible to note that the introduction of ions onto the graphene surface led to significant variations in the electronic parameters.

Table 2. HOMO, LUMO, and Fermi level of GQD, GQD#$Li^+$ , GQD#$Na^+$, and GQD#$K^+$.

| | GQD | GQD#$Li^+$ | GQD#$Na^+$ | GQD#$K^+$ |
|---|---|---|---|---|
| HOMO (eV) | -6.20 | -8.84 | -8.70 | -8.61 |
| LUMO (eV) | -1.52 | -4.19 | -4.06 | -3.96 |
| Fermi level (eV) | -3.86 | -6.52 | -6.38 | -6.28 |

Source: Authors.

The electron density surfaces for the HOMO and LUMO orbitals of the materials GQD, GQD#$Li^+$, GQD#$Na^+$, and GQD#$K^+$ are presented in **Figure 2.**

Figure 2. Orbitals of (a) HOMO - GQD, (b) LUMO - GQD, (c)HOMO - GQD#$Li^+$, (d) LUMO - GQD#$Li^+$, (e) HOMO - GQD#$Na^+$, (f) LUMO - GQD#$Na^+$, (g) HOMO - GQD#$K^+$, and (h) LUMO - GQD#$K^+$.

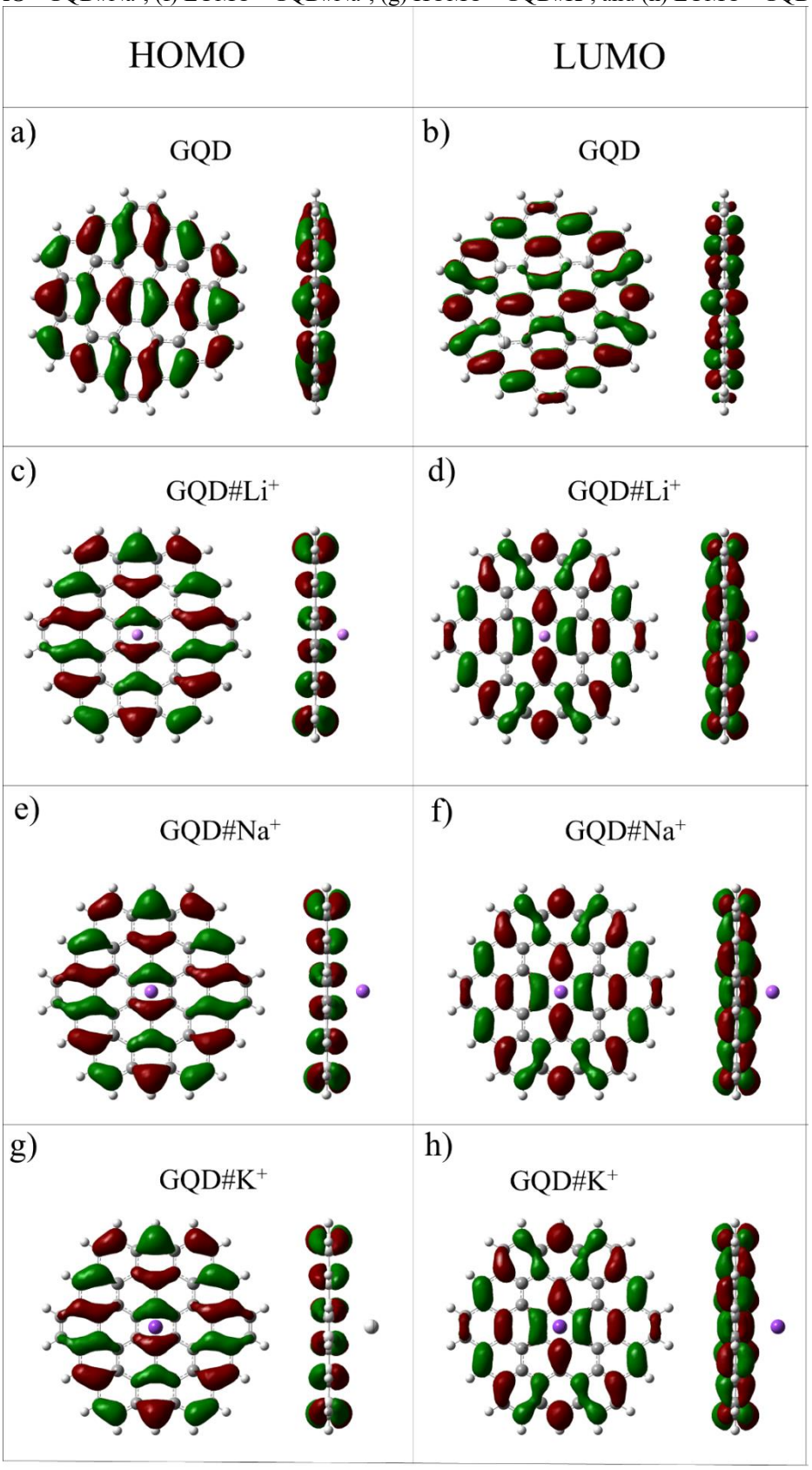


Source: Authors.

The image depicts a graphene surface with an ion positioned above the central hexagonal ring. Carbon and edge hydrogen atoms are shown in gray, while green and red regions indicate areas of high and low electron density, respectively. Lithium, sodium, and potassium ions are represented in violet. Comparing the electron density surface for the HOMO orbital, the GQD surface exhibits a uniform distribution of electron density across the entire structure, as shown in **Figure 2 (a)**. The HOMO orbital of graphene surfaces containing the positive ions $Li^+$, $Na^+$, and $K^+$ exhibits a region of lower electron density near the ion and higher electron density on the graphene surface, due to electron transfer between the ion and the graphene surface (ZHAO *et al*., 2018), as shown in **Figures 2 (c), (e), and (g)**, respectively. **Figures 2 (b), (d), (f),** and **(h)** show the electron density distribution patterns for the LUMO orbital of GQD, GQD#$Li^+$, GQD#$Na^+$, and GQD#$K^+$, respectively. GQD exhibits a uniformly distributed electron density across the entire surface. The GQD containing positive ions, $Li^+$, $Na^+$, and $K^+$, demonstrates regions of higher electron density on the graphene surface near the ions, which can be attributed to charge transfer between the ions and the graphene surface (ZHAO *et al*., 2018).

## CONCLUSIONS

In this work, DFT-based simulations were employed to investigate, at both vibrational and electronic levels, the effects of $Li^+$, $Na^+$, and $K^+$ adsorption on the structural, spectroscopic, and electronic properties of graphene quantum dots. The variations observed in the D and G Raman bands, as well as in the ID/IG disorder ratio, demonstrated that ion–surface interactions induce subtle but systematic structural perturbations, consistent with trends reported in *operando* Raman studies of carbon-based materials. Among the investigated systems, GQD#$Li^+$ exhibited the most pronounced Raman shifts, the strongest adsorption energy, and the largest modifications in electronic parameters, highlighting lithium as the most effective cation in promoting charge redistribution and electronic reorganization at the GQD surface.

The analysis of frontier orbitals and electron density maps revealed the fundamental mechanism governing the vibrational behavior: charge transfer from the cation to the GQD followed by electrostatic stabilization, which modifies the HOMO, LUMO, and Fermi levels and directly influences Raman-active phonon modes. The strong agreement between simulated results and experimental tendencies observed in polarized carbon electrodes reinforces the validity of the computational model and confirms the predictive capacity of DFT in describing ion-induced

doping, adsorption mechanisms, and vibrational modulation.

Overall, the results indicate that alkali cation adsorption is an effective strategy for tuning the electronic and vibrational properties of graphene quantum dots. Among the studied materials, GQD#$Li^+$ emerges as the most promising candidate for applications in energy storage devices, electrochemical sensors, and charge-modulated nanosystems. The findings presented here provide valuable insights for the rational design of functionalized carbon nanomaterials and offer a solid foundation for interpreting *operando* Raman spectroscopy in complex electrochemical environments.

## REFERENCES

BA, E. C. T. *et al*. Deconvolution process approach in Raman spectra of DLC coating to determine the sp3 hybridization content using the ID/IG ratio in relation to the quantification determined by X-ray photoelectron spectroscopy. **Diamond and Related Materials**, v. 122, p. 108818, fev. 2022. Available at: https://doi.org/10.1016/j.diamond.2021.108818, Accessed on: Sept. 27, 2025.

CAI, P.; ZOU, K.; *et al*. Comprehensive Understanding of Sodium-Ion Capacitors: Definition, Mechanisms, Configurations, Materials, Key Technologies, and Future Developments. **Advanced Energy Materials**, v. 11, n. 16, 10 abr. 2021. Available at: https://doi.org/10.1002/aenm.202003804, Accessed on: Sept. 14, 2025.

CAI, P.; MOMEN, R.; *et al*. Functional carbon materials processed by NH3 plasma for advanced full-carbon sodium-ion capacitors. **Chemical Engineering Journal**, v. 420, p. 129647, set. 2021. Available at: https://doi.org/10.1016/j.ce.2021.129647, Accessed on: Oct. 10, 2025.

CAPELLE, K. A bird's-eye view of density-functional theory. **Brazilian Journal of Physics**, v. 36, n. 4a, p. 1318–1343, dez. 2006. Available at: https://doi.org/10.1590/S0103-97332006000700035, Accessed on: Jan. 3, 2025.

CHMIOLA, J. *et al*. Monolithic Carbide-Derived Carbon Films for Micro-Supercapacitors. **Science**, v. 328, n. 5977, 23 abr. 2010. Available at: https://doi.org/10.1126/science.1184126, Accessed on: Dec. 15, 2024.

COMPAGNINI, G. *et al*. Ion beam induced defects in graphene: Raman spectroscopy and DFT calculations. **Journal of Molecular Structure**, v. 993, n. 1–3, p. 506–509, maio 2011. Available at: https://doi.org/10.1016/j.molstruc.2010.12.065, Accessed on: Oct. 27, 2025.

DAVID S. SHOLL; JANICE A. STECKEL. **Density Functional Theory: A Practical Introduction**. [S.l.]: John Wiley & Sons, 2009. Available at: https:// onlinelibrary.wiley.com, Accessed on: Sept. 27, 2025.

DENG, X. *et al*. High content anion (S/Se/P) doping assisted by defect engineering with fast

charge transfer kinetics for high-performance sodium ion capacitors. **Science Bulletin**, v. 66, n. 18, p. 1858–1868, set. 2021. Available at: https://doi.org/10.1016/j.scrib.2021.04.042, Accessed on: Jul. 13, 2025.

FERRARI, A. C.; BASKO, D. M. Raman spectroscopy as a versatile tool for studying the properties of graphene. **Nature Nanotechnology**, v. 8, n. 4, p. 235–246, 4 abr. 2013. Available at: https://doi.org/10.1038/nnano.2013.46, Accessed on: Sept. 26, 2025.

FRISCH, M. J. *et al*. **Gaussian 09,** . . [S.l.]: Gaussian, Inc. , 2009. Available at: https://gaussian.com, Accessed on: Mar. 21, 2025.

FRISCH, Michael J.; POPLE, J. A.; BINKLEY, J. S. Self-consistent molecular orbital methods 25. Supplementary functions for Gaussian basis sets. **The Journal of Chemical Physics**, v. 80, n. 7, p. 3265–3269, 1 abr. 1984. Available at: https://doi.org/10.1063/1.447079, Accessed on: Nov. 5, 2025.

GUO, R. *et al*. Functionalized carbon dots for advanced batteries. **Energy Storage Materials**, v. 37, p. 8–39, maio 2021. Available at: https://doi.org/10.1016/j.ensm.2021.01.020, Accessed on: Jun. 26, 2025.

HONG, J. *et al*. Origin of New Broad Raman D and G Peaks in Annealed Graphene. **Scientific Reports**, v. 3, n. 1, p. 2700, 19 set. 2013. Available at: https://doi.org/10.1038/srep02700, Accessed on: Oct. 14, 2025.

KASHINSKI, D. O. *et al*. Harmonic Vibrational Frequencies: Approximate Global Scaling Factors for TPSS, M06, and M11 Functional Families Using Several Common Basis Sets. **The Journal of Physical Chemistry A**, v. 121, n. 11, p. 2265–2273, 23 mar. 2017. Available at: https://doi.org/10.1021/acs.jpca.6b1214, Accessed on: Oct. 14, 2025.

KOHN, W.; SHAM, L. J. Self-Consistent Equations Including Exchange and Correlation Effects. **Physical Review**, v. 140, n. 4A, p. A1133–A1138, 15 nov. 1965. Available at: https://doi.org/10.1103/PhysRev.140.A1133, Accessed on: Sept. 27, 2025.

LEE, J. W. *et al*. A Facile and Template-Free Hydrothermal Synthesis of Mn3O4 Nanorods on Graphene Sheets for Supercapacitor Electrodes with Long Cycle Stability. **Chemistry of Materials**, v. 24, n. 6, 27 mar. 2012. Available at: https://doi.org/10.1021/cm203697w, Accessed on: Jun. 17, 2025.

LI, Lin *et al*. Kilogram-Scale Synthesis and Functionalization of Carbon Dots for Superior Electrochemical Potassium Storage. **ACS Nano**, v. 15, n. 4, p. 6872–6885, 27 abr. 2021. Available at: https://doi.org/10.1021/acsnano.0c10624, Accessed on: May. 27, 2025.

LI, Linlin *et al*. Electrospun Porous NiCo2O4 Nanotubes as Advanced Electrodes for Electrochemical Capacitors. **Chemistry – A European Journal**, v. 19, n. 19, 3 maio 2013. Available at: https://doi.org/10.1002/chem.201204153, Accessed on: Nov. 14, 2025.

LIU, J. *et al*. The Dependence of Graphene Raman D-band on Carrier Density. **Nano Letters**, v. 13, n. 12, p. 6170–6175, 11 dez. 2013. Available at: https://doi.org/10.1021/nl4035048,

Accessed on: Jun. 7, 2025.

LIU, W. *et al*. Graphene Quantum Dots-Based Advanced Electrode Materials: Design, Synthesis and Their Applications in Electrochemical Energy Storage and Electrocatalysis. **Advanced Energy Materials**, v. 10, n. 29, 22 ago. 2020. Available at: https://doi.org/10.1002/aenm.202001275, Accessed on: Dec. 22, 2024.

LU, T.; CHEN, F. Multiwfn: A multifunctional wavefunction analyzer. **Journal of Computational Chemistry**, v. 33, n. 5, p. 580–592, 15 fev. 2012. Available at: https://doi.org/10.1002/jcc.22885, Accessed on: Aug. 15, 2025.

MADITO, M. J. Correlation of the Graphene Fermi-Level Shift and the Enhanced Electrochemical Performance of Graphene-Manganese Phosphate for Hybrid Supercapacitors: Raman Spectroscopy Analysis. **ACS Applied Materials & Interfaces**, v. 13, n. 31, 11 ago. 2021. Available at: https://doi.org/10.1021/acsami.1c07104, Accessed on: Dec. 22, 2024.

MALARD, L. M. *et al*. Raman spectroscopy in graphene. **Physics Reports**, v. 473, n. 5–6, p. 51–87, abr. 2009. Available at: https://doi.org/10.1016/j.physrep.2009.02.003, Accessed on: Sept. 13, 2025.

PATTARAPONGDILOK, N.; PARASUK, V. Adsorptions of lithium ion/atom and packing of Li ions on graphene quantum dots: Application for Li-ion battery. **Computational and Theoretical Chemistry**, v. 1177, p. 112779, maio 2020. Available at: https://doi.org/10.1016/j.comptc.2020.112779, Accessed on: Oct. 14, 2025.

RABELO, C. *et al*. Micro- and Nano-Raman Spectroscopy Characterization of Exfoliated Graphene with Helium-Ion Microscope Patterned Line Defects. **physica status solidi (b)**, v. 260, n. 12, 4 dez. 2023. Available at: https://doi.org/10.1002/pssb.202300204, Accessed on: Oct. 27, 2025.

SIMON, P.; GOGOTSI, Y. Perspectives for electrochemical capacitors and related devices. **Nature Materials**, v. 19, n. 11, 3 nov. 2020. Available at: https://doi.org/10.1038/s41563-020-0747-z, Accessed on: Sept. 27, 2025.

TAYYAB, M. *et al*. Band-gap tuning of graphene by Mg doping and adsorption of Br and Be on impurity: A DFT study. **Computational Condensed Matter**, v. 23, p. e00469, jun. 2020. Available at: https://doi.org/10.1016/j.cocom.2020.e00469, Accessed on: Jun. 15, 2025.

TUNG, T. T. *et al*. Irradiation methods for engineering of graphene related two-dimensional materials. **Applied Physics Reviews**, v. 10, n. 3, 1 set. 2023. Available at: https://doi.org/10.1063/5.0148376, Accessed on: Jun. 18, 2025.

VENÂNCIO, R. *et al*. Combining electrochemical, molecular simulation and operando techniques to investigate the stability of electrodes and organic electrolytes used in EDLCs. **Energy Storage Materials**, v. 62, p. 102943, set. 2023. Available at: https://doi.org/10.1016/j.ensm.2023.102943, Accessed on: Jul. 17, 2025.

VENÂNCIO, R. *et al*. In-situ electrochemical and operando Raman techniques to investigate

the effect of porosity in different carbon electrodes in organic electrolyte supercapacitors. **Journal of Energy Storage**, v. 50, p. 104219, jun. 2022. Available at: https://doi.org/10.1016/j.est.2022.104219, Accessed on: Jul. 19, 2025.

VICENTINI, R.; VENÂNCIO, R.; *et al*. New Insights on the Sodium Water-in-Salt Electrolyte and Carbon Electrode Interface from Electrochemistry and Operando Raman Studies. **ACS Applied Materials & Interfaces**, v. 13, n. 51, p. 61139–61153, 29 dez. 2021. Available at: https://doi.org/10.1021/acsami.1c1877, Accessed on: Sept. 27, 2025.

VICENTINI, R.; DA SILVA, L. M.; *et al*. Raman probing carbon & aqueous electrolytes interfaces and molecular dynamics simulations towards understanding electrochemical properties under polarization conditions in supercapacitors. **Journal of Energy Chemistry**, v. 60, p. 279–292, set. 2021. Available at: https://doi.org/10.1016/j.jechem.2021.01.003, Accessed on: Sept. 14, 2025.

WANG, H. *et al*. One-step strategy to three-dimensional graphene/VO2 nanobelt composite hydrogels for high performance supercapacitors. **J. Mater. Chem. A**, v. 2, n. 4, 2014. Available at: https://doi.org/10.1039/C3TA13932H, Accessed on: Apr. 08, 2025.

WANG, Y. ying *et al*. Raman Studies of Monolayer Graphene: The Substrate Effect. **The Journal of Physical Chemistry C**, v. 112, n. 29, p. 10637–10640, 1 jul. 2008. Disponível em: Available at: https://doi.org/10.1021/jp8008404, Accessed on: May. 27, 2025.

WEAVING, J. S. *et al*. Elucidating the Sodiation Mechanism in Hard Carbon by Operando Raman Spectroscopy. **ACS Applied Energy Materials**, v. 3, n. 8, p. 7474–7484, 24 ago. 2020. Available at: https://doi.org/10.1021/acsaem.0c00867, Accessed on: Aug. 13, 2025.

WU, J.-B. *et al*. Raman spectroscopy of graphene-based materials and its applications in related devices. **Chemical Society Reviews**, v. 47, n. 5, p. 1822–1873, 2018a. Available at: https://doi.org/10.1039/C6CS00915H, Accessed on: Oct. 27, 2025.

XIAO, J.; MOMEN, R.; LIU, C. Application of carbon quantum dots in supercapacitors: A mini review. **Electrochemistry Communications**, v. 132, p. 107143, nov. 2021. Available at: https://doi.org/10.1016/j.elecom.2021.107143, Accessed on: Aug. 15, 2025.

XU, H. *et al*. Effect of Graphene Fermi Level on the Raman Scattering Intensity of Molecules on Graphene. **ACS Nano**, v. 5, n. 7, p. 5338–5344, 26 jul. 2011. Available at: https://doi.org/10.1021/nn103237x, Accessed on: Aug. 15, 2025.

YANAI, T.; TEW, D. P.; HANDY, N. C. A new hybrid exchange–correlation functional using the Coulomb-attenuating method (CAM-B3LYP). **Chemical Physics Letters**, v. 393, n. 1–3, p. 51–57, jul. 2004. Available at: https://doi.org/10.1016/j.cplett.2004.06.011, Accessed on: Oct. 14, 2025.

ZHANG, Z. *et al*. Facile Synthesis of 3D MnO2 –Graphene and Carbon Nanotube–Graphene Composite Networks for High-Performance, Flexible, All-Solid-State Asymmetric Supercapacitors. **Advanced Energy Materials**, v. 4, n. 10, 17 jul. 2014. Available at: https://doi.org/10.1002/aenm.201400064, Accessed on: May. 27, 2025.

ZHAO, S. *et al*. Self-assembled hierarchical porous NiMn2O4 microspheres as high performance Li-ion battery anodes. **RSC Advances**, v. 8, n. 73, 2018. Available at: https://doi.org/10.1039/C8RA08080A, Accessed on: Apr. 08, 2025.

ZOU, K. *et al*. Revealing dual capacitive mechanism of carbon cathode toward ultrafast quasi-solid-state lithium ion capacitors. **Journal of Energy Chemistry**, v. 60, p. 209–221, set. 2021. Available at: https://doi.org/10.1016/j.jechem.2020.12.039, Accessed on: Sept. 27, 2025.